Holocene rapid (decades) multi-metre marine transgressions by climatically driven Antarctic ice-collapse events. Another event imminent?

Manuscript version 1, 19th March 2025

Roger Higgs, Geoclastica Ltd, UK

rogerhiggs@hotmail.com https://orcid.org/0000-0002-4827-9704

Abstract

The controversial 1961 'Fairbridge Curve' of Holocene global sea-level (SL), showing metre-scale (to ~5m) oscillations based on carbon-dated geological index points (SL 'benchmarks''), is vindicated by syntheses (companion-articles by present author) of the literature on: (1) Holocene sea level, exposing flawed assumptions and methods in constructing *non*-oscillating SL curves; and (2) English *archaeology*, its SL significance previously underappreciated, revealing a ~4m SL rise that spanned only ~70 years (~430-500AD), equating to Fairbridge's 'Rottnest transgression', but far better-dated (dendrochronology, coins, pottery). The present contribution, a review of polar glaciological literature, argues that 'Fairbridge-type', large (m), rapid (decades) SL rises result from Antarctic 'MICI' ice-cliff-collapse events. The Rottnest rise (began ~430AD) is attributed here to a 12-year Arctic warm spike (Sun-driven?) that peaked 402AD; the 30-year lag is the delay for downwelling 'overwarmed' Arctic sea-surface water to reach Antarctica by 'conveyor-belt' ocean circulation. Since 2005, anthropogenically-boosted Arctic average temperature has continuously exceeded the ~402AD peak, portending another MICI-driven rise, starting by ~2035 (2005 plus lag), likely to raise SL at least 3m by ~2100. Closely monitored Antarctic glaciers indeed show signs of approaching failure. On the Fairbridge Curve, each SL rise is closely followed by a SL fall of similar magnitude, probably intrinsic to the MICI process.

1. Introduction

Throughout this article, the following abbreviations are used: mm = millimetres; cm = centimetres; m = metres; y = years; ky = thousand years; ka = thousand years B.P. ('Before Present', i.e. before 1950, by convention).

The Intergovernmental Panel on Climate Change (IPCC) is confident that, due to anthropogenic global warming, sea level (SL) will rise >0.5 and <1m by 2100, with a "Low-likelihood, high-impact" worst case of 1.75m (IPCC, 2021, fig. SPM.8d). In contrast, evidence gathered from exhaustive reviews of the literature on (1) Holocene SL and (2) English coastal archaeology, assessed from the author's sedimentological perspective, strongly suggests that the rise will be at least 3m (Higgs, 2024, 2025a, b). Those syntheses vindicate the controversial 1961 "Fairbridge Curve" (Fairbridge, 1976, p. 358 and fig. 3) of Holocene interglacial period (11.7ka to present-day; Walker et al., 2009) SL, with its metre-scale (up to ~5m) oscillations based on loosely carbon-dated geological index points (SL 'benchmarks'') around the world. The archaeology review (Higgs, 2025b) reveals a ~4m SL rise in only ~70 years (~430-500AD), equating to Fairbridge's global 'Rottnest transgression', but much more tightly dated (dendrochronology, coins, pottery). The present contribution, a synthesis of polar glaciological literature, argues that Antarctic 'MICI' ice-cliff-collapse events are the only viable cause of 'Fairbridge-type', large (m), rapid (decades) SL rises.

2. Cause of Rottnest Transgression: Antarctic ice collapse?

The only plausible driver of a global SL rise as large and fast as the Rottnest (and probably all other Fairbridge-type SL rises) is an Antarctic and/or Greenland ice-collapse event at one or more marine-terminating glaciers (i.e. grounded below SL), by hypothetical "Marine Ice Sheet Instability" (MISI) and/or "Marine Ice Cliff Instability" (MICI; DeConto and Pollard, 2016). In a MISI event, upwelling ocean water of abnormal warmth intrudes under a glacier's floating ice-shelf, increasing the rate of melting at the grounding line and the shelf's underside, causing the grounding line to retreat and the ice-shelf to thin and shorten (DeConto and Pollard, 2016, fig. 2a-c). If retreat occurs on a retrograde (landward-dipping) bedrock slope, the ice thickness at the grounding line continually increases. This thickening, and the simultaneous melt-driven shrinkage of the ice shelf (lessening its glacier-buttressing effect), cause accelerating ice flow across the grounding line, such that ice is transferred from the *grounded* glacier to the *floating* shelf (continually melting and calving), thereby raising world SL. Glacier acceleration continues in a "positive runaway feedback" (DeConto and Pollard, 2016, fig. 1c) until the grounding line reaches a prograde bedslope (Deconto and Pollard, 2016), or until some other mechanism arrests the MISI (see below).

A MISI possibly evolves into a MICI event (Wise et al., 2017), in which the glacier front liberates an iceberg "armada", raising SL (Jakobsson et al., 2011, fig. 4c). MICI is theorized as restricted to marine-terminating glaciers which have (a) completely lost their protective ice shelves (by melting and enhanced calving due to a warming ocean and atmosphere), producing an ice cliff at the grounding line; and (b) receded on a retrograde bedslope until the grounding line is ~700m below SL, such that the cliff is ~800m tall (i.e. ~100m of ice above the water line; DeConto and Pollard, 2016, fig. 2f). At this point, "the stresses at the cliff face exceed the strength of the ice, and the cliff fails structurally in repeated calving events" (IPCC, 2019, fig. CB8.1). The cliff becomes ever-higher as it retreats into progressively thicker ice (DeConto and Pollard, 2016, fig. 2), increasing the calving rate. The "retreat would continue unabated until temperatures cooled enough to reform a buttressing ice shelf, or the ice margin retreated onto bed elevations too shallow to support the tall, unstable cliffs" (DeConto and Pollard, 2016, p. 592), requiring an inboard prograde slope (cf. Pattyn, 2018).

No glacier is currently known to be undergoing MICI retreat. The "closest analog ... might be the separation and overturning of km-scale bergs as observed currently at Jakobshavn and Helheim glaciers" (Pollard et al., 2015, p. 117) in Greenland, "in water depths of ~700m to 1000m with no contiguous ice shelves" (p. 114). At Jakobshavn, constrained in a V-shaped valley only ~6km wide at the top (An et al., 2017, figs 1, 2), "the cliff... may be partially supported by back stress from the glacier sides [valley walls] or its ice mélange" (Pollard et al., 2015, p. 117) floating in front, choking the fjord. Either (or both) of these processes potentially restrains calving at the ice cliff. Jakobshavn contributes only ~0.1mm/y to modern SL rise (Bondzio et al., 2018). Helheim is equally narrow and fronted by mélange (Straneo et al., 2016, fig. 2). In Antarctica, Crane Glacier may or may not have undergone a MICI episode immediately after the buttressing Larsen B Ice Shelf collapsed in 2002 (Needell and Holschuh, 2023).

Crane's grounding line is ~900m deep (Rebesco et al., 2014, fig. 1B), but the glacier is confined in an even narrower (~3.5km) valley, choked with mélange (GoogleEarth).

The observation that Rottnest- and other Fairbridge-type SL rises are of finite amplitude (metres) and duration (decades to perhaps centuries) (Higgs, 2025a) implies that the causative MISI and/or MICI event must eventually stop, far short of collapsing the entire Greenland and/or Antarctic ice sheet, which would raise SL by ~7m and ~58m respectively (Morlighem et al., 2017, 2020). What is the MISI/MICI 'braking' mechanism? Hypothetically, upon encountering a prograde slope, MISI ice-flow into the ocean should decelerate (DeConto and Pollard, 2016), the timing varying among glaciers, depending on their basal topography. Another potential limiting mechanism is arrival of cooler ocean water intruding below the shelf, allowing the shelf to regrow, increasing back-stress on the glacier, eventually arresting the MISI. A third, intrinsic, 'Antarctic see-saw' mechanism can be envisaged, as follows. Inevitable bedrock isostatic uplift (with a time-lag), due to glacier retreat, may cause the ice shelf to reground on shelf ridges (Bradley et al., 2015). Shelf grounding would increase its buttressing effect, causing the glacier to decelerate and therefore thicken, advancing the grounding line (cf. Kingslake et al., 2018, extended data fig. 3). Resulting renewal of subsidence would deepen the shelf, enhancing ocean-water intrusion, such that the next 'flush' of warmer-than-usual water would renew the cycle. Two potential mechanisms for halting a *MICI* event are: (1) glacier acceleration and rapid thinning, reducing the ice-cliff height to below the MICI threshold (Morlighem et al., 2024); and (2) grounding-line retreat onto a prograde slope, again lowering the cliff.

Numerous modelling experiments simulating a circum-Antarctic MISI event (without MICI) predicted a SL rise ranging from ~1 to ~7m within 100y (Sun et al., 2021, fig. 1c), consistent with the proposed Rottnest rise of ~4m in ~70y (Higgs, 2024, 2025b). However, many of the modelled variables have very high uncertainty (Sun et al., 2021). According to Needell and Holschuh (2023, p. 1), the "fastest projected rates of sea level rise appear in models which include ... MICI"; and "during several periods in Earth's history, ice sheet models have difficulty reproducing the observed rapid sea level rise without it". Thus, it seems probable that MICI (perhaps preceded by MISI) caused the Rottnest transgression. MICI also appears better able than MISI to explain the intrinsic(?) SL fall following each Fairbridge-type rise (see Section 4). Persuasive

Antarctic sea-bed evidence for at least two MICI events, one near the start of Holocene time and one intra-Holocene, has been documented (see below).

If the Rottnest ice-collapse event was indeed by MICI, it must have been confined largely or entirely to Antarctica. Of Greenland's ice sheet, which feeds ~200 marine-terminating glaciers (Rignot and Mouginot, 2012), the total area with basement deeper than 700m (MICI threshold) is <1%, comprising about six glaciers (including Jakobshavn but not Helheim), all confined in narrow (<10km) bedrock valleys (Morlighem et al., 2017, fig. 2) likely to impede ice-cliff collapse (see above), a configuration that presumably applied equally to Rottnest time, only ~1.5ky ago. Moreover, a ~4m (Rottnest) SL rise *not* involving Antarctica would require melting of about half (54%) of Greenland's ice-sheet volume (~7m sea-level equivalent; Morlighem et al., 2017), yet there is no evidence, in ice cores or at outcrop, for such a drastic deglaciation so recently. In contrast, Antarctica's ice sheet has eight times the area and ten times the volume of Greenland's. At least 5% of the area has basement >700m below SL, including more than ten marine-terminating glaciers with grounding lines individually 10-70km wide (transverse to flow), totalling >200km (see below; Morlighem et al., 2020, figs 1, 2). In addition, glaciers vulnerable to MISI (retrograde bed) exist at multiple locations around Antarctica, concentrated in West Antarctica (e.g. Sun et al. 2021, fig. 4).

Possible evidence for a recent MICI event is seen in multibeam-sonar images from deep water (~600-900m) in glacially formed Pine Island Trough, which runs seaward across the continental shelf in front of Pine Island- and Thwaites Glaciers, West Antarctica. The images show interpreted iceberg-keel ploughmarks of two distinct kinds, here called Types 1 and 2. Type 1 ploughmarks are laterally-merged furrows, overprinted by transverse, symmetrical, "corrugation ridges" (Jakobsson et al., 2011). Ridge amplitude (0.3-3m) and crest-spacing (50-300m) vary rhythmically (Jakobsson et al., 2011). The furrows, occupying the entire 30-by-15km area of a published image (Jakobsson and Anderson, 2016, fig. 1a), are nearly straight and individually ~200-500m wide. In the image's northern and eastern sectors, which average ~50m shallower, the furrows are only faintly discernible, as they are almost entirely overprinted by a mass of Type 2 ploughmarks, which are narrow (~50-200m), multi-directional, cross-cutting, and curving or jagged (with multiple kinks, including 'hooks'). Some Type 2 ploughmarks appear to show transverse 'stripes' (near the resolution limit of Jakobsson and Anderson, 2016, fig. 1a, b), suggesting that they too are corrugated. Other Type 2 ploughmarks occur ~80km southward (shoreward) along Pine Island Trough (Wise et al., 2017; compare fig. 1b northern and fig. 1c southern ploughmarks).

Type 1 ploughmarks were ascribed by Jakobsson et al. (2011, 2012) to a cluster of thick (tall) icebergs, comprising the innermost ice shelf, broken off at the grounding line after the rest of the shelf had disintegrated (Jakobsson et al., 2011, fig. 4; republished in Jakobsson and Anderson, 2016, fig. 1d). The cluster was either intrinsically stable (too wide to capsize) or was propped upright in a thinner "floating canopy of ice, most likely a thick armada of icebergs from a collapsing ice shelf" (p. 693). The cluster drifted offshore at least 30km (minimum lengthwise extent of the furrows in Jakobsson and Anderson, 2016, fig. 1a) until it grounded on the seaward-shallowing seabed; then it continued shuffling upslope (enabled by gradual thinning by underwater melting), rhythmically rising and descending on the tide, each descent causing sediment to extrude at the cluster's trailing edge, forming a corrugation ridge (Jakobsson et al., 2011, fig. 4C). The Jakobsson model of corrugated-furrow development is one of various possible origins discussed by Graham et al. (2013, 2016).

Type 2 ploughmarks were attributed explicitly to MICI ice-cliff failure by Wise et al. (2017; co-author Jakobsson), producing tall, "pinnacle-shaped", downward-tapering icebergs, wide enough to avoid capsizing, liberated singly (their fig. 4b) and thus free to drift independently. In sonar swaths, Wise et al. (2017, extended data fig. 1) mapped a huge number (10,831) of Type 2 ploughmarks (many probably reflect individual icebergs drifting back and forth across each swath, and travelling from one swath to another). The interpreted MICI event began ~12.3ka and ended before ~11.2ka (Wise et al., 2017, fig. 4), i.e. near the start of Holocene time.

A revised model for Types 1 and 2 ploughmarks is offered here, modifying and integrating the above interpretations, as follows. After a period of ice-shelf disintegration, the final (innermost, thickest) ice-shelf remnant broke off at the grounding line, as envisaged by Jakobsson et al. (2011, 2012), producing a tall mega-iceberg (cf. their *cluster* of bergs), wide enough to not capsize (Wise et al., 2017). The glacier front, now an ice cliff, was taller (>~800m) than the MICI threshold, initiating runaway ice-cliff collapse, forming a mélange of thinner bergs that helped to push the mega-berg outward and into contact with the offshore-shallowing seabed, forming Type 1 corrugated furrows in the manner invoked by Jakobsson et al. (2011). Thus, Type 1 ploughmarks are a MICI 'smoking gun'. With time, by surface- and underwater melting, the mega-berg disaggregated (along crevasses) into narrower and thinner (less-tall) pinnacles. By then, the ice mélange at this location, increasingly distant from the retreating (by MICI) ice cliff, was sufficiently dispersed and thinned (by melting), at least seasonally, to enable pinnacle bergs, driven by wind and tides, to wander freely, emplacing Type 2 ploughmarks, except in those parts of Type 1 regions too deep to re-plough.

Seabed corrugations "virtually identical" (Jakobsson et al., 2011, p. 692) to those of Pine Island Trough have been imaged on the Ross shelf of West Antarctica and on the East Antarctic sector of the Weddell shelf (references in Jakobsson et al., 2011); their "pervasive occurrence suggests a common mechanism and explanation for their origin" (p. 692). The widespread occurrence of corrugations accords with the idea (below) of simultaneous MICI collapse at numerous glaciers, causing modest (km?) glacier-snout retreat at each glacier, collectively and rapidly (decades) raising world SL by a few metres each time (Fairbridge-type transgressions).

The foregoing examples of corrugations are all in open water. However, ~300km landward of the above example in Pine Island Bay, essentially identical corrugations, again overprinting laterally amalgamated longitudinal troughs interpreted as ploughmarks, exist on a basement ridge under Pine Island Ice Shelf (Graham et al., 2013). If these corrugations reflect a MICI event (requiring removal of the ice shelf), the grounding line (at the ice cliff) must have been near its present-day position but, by definition, without an ice shelf in front of it. The sub-shelf corrugations possibly pertain to the Rottnest MICI. Alternatively, these corrugations may reflect a previous Holocene MICI event (causing one of Fairbridge's earlier transgressions). If so, Rottnest corrugations were possibly formed farther inboard, at a more-receded ice front, only to be erased by grounding-line readvance (see below for evidence for Late Holocene glacier readvance).

Graham et al. (2013) preferred an alternative origin for the Pine Island sub-shelf corrugations, by rhythmic (tidal) ice-*shelf*-keel grounding, because the Jakobbson iceberg model (above) would imply "a much reduced calving front", inboard of Graham's corrugations, for which there was "thus far, no independent evidence" (their p. 1362; but see below for discussion of possible retreat and readvance of Pine Island Glacier in the last 5ky). Casting doubt on the Graham et al. model, in order to reconcile sub-shelf corrugation spacing with modern ice-shelf seaward-flow rates, they had to interpret each corrugation as representing the peak of the 14-day spring-neap cycle, unlike the Jakobsson et al. (2011) open-sea corrugations (above), in which every 14th corrugation tends to be the highest, suggesting that each corrugation represents one day.

Corrugation ridges of similar geometry and rhythmicity, but much lower spacing (<10m) and amplitude (10s cm), have also been observed in front of Thwaites Glacier, where they are attributed to tidal flexure of a retreating grounding line (Graham et al., 2022, including supplementary; Hogan et al., 2023).

Whichever Antarctic glacier was the first to lose its ice shelf and begin retreating by MICI, the resulting initial SL rise would have destabilised other glaciers' remaining ice shelves (by tidal flexure), hastening their disintegration and MICI onset. The question arises, how far did each contributing glacier recede before the MICI event ended? Braddock et al. (2022, p. 568) concluded that "Thwaites and Pine Island glaciers have not been *substantially* [emphasis added] smaller than present during the past 5.5kyr", based on a relative-SL graph (their fig. 3a) compiled from raised (by isostatic rebound), carbon-dated beaches near these glaciers. The SL curve is said to preclude any change (decrease) in the rate of uplift "that would characterize *large-scale* [emphasis added] ice re-expansion" following a retreat event, although "we cannot preclude *minor* [emphasis added] grounding-line fluctuations" (p. 568). Unfortunately, the authors did not quantify "substantially", "large-scale" or "minor"; perhaps a retreat and re-expansion of, say, <10km is beyond the resolution of their SL curve. The curve, interpolated among the data-points, is smooth rather than oscillating (therefore included in Table 2 of Higgs, 2025a). However, the sample gaps, error-bars, and 2-sigma uncertainty-band allow m-scale SL oscillations, including the Rottnest. The Braddock curve indicates ~10m of relative SL fall between 4 and 1ka (i.e. average rate 3.5mm/y; p. 570). Thus, a (Rottnest) 4m rise lasting 70y (i.e. ~57mm/y average) would ideally (given enough data points and zero age/elevation errors) appear on the curve as a 3.8m reversal (net 54mm/y), and a 3m rise as a 2.8m reversal. In fact, the age- and elevation error-bars of the data-points permit a Rottnest-age (~430-500AD) reversal of up to 1.9m (see cluster of overlapping data-points on the Braddock fig. 3a SL curve). The shortfall may indicate that the data-points' estimated elevation uncertainty (0.3 to 0.7m; Braddock et al. 'Methods') is, in fact, larger.

A different technique, cosmic-ray exposure-dating of glacially transported erratic cobbles and ice-scoured bedrock surfaces, is permissive of glacier retreat and readvance in the Pine Island Glacier (PIG)-Thwaites Glacier region in the last 5ky (Johnson et al., 2022, fig. 2) and elsewhere (see below). Exposure ages at a former PIG-tributary glacier (retreated; no longer connected to PIG) revealed a rapid glacier-thinning event at ~8ka lasting "several decades, and possibly centuries" (Johnson et al., 2014, p. 1000), consistent with a Fairbridge-type SL rise pre-dating the Rottnest. At Mackay Glacier in East Antarctica, rapid upstream thinning ~7ka, lasting at least 250y, was attributed to a MISI (sic) event by Jones et al. (2015), before the MICI concept became well known (Pollard et al., 2015; DeConto and Pollard, 2016).

Consistent with the idea that Rottnest- and other Fairbridge-type SL rises reflect MICI events occurring simultaneously at numerous glaciers, multiple techniques (satellite imagery; ice-penetrating radar; exposure ages; GPS; ice temperature vs depth) employed on both the West- and East Antarctic flanks of the Ross and Weddell embayments collectively suggest Middle- or Late Holocene glacier retreat behind the modern grounding line by up to as much as 200km (sic), followed by Late Holocene re-advance (Bindschadler et al., 1990; Siegert et al., 2013, 2019; Bradley et al., 2015; Johnson et al., 2022). Such a large retreat would inevitably have generated a global SL rise. Another technique, carbon-dating of subglacial sediment cores in the Ross Sea embayment, indicates grounding line retreat, at some time(s) during the Holocene, "several hundred kilometres inland of today's grounding line, before isostatic rebound caused it to re-advance to its present position" (Kingslake et al., 2018, p. 1). Due to the low resolution of these techniques, they are possibly detecting the cumulative effect of *several* Middle and Late Holocene MICI rapid retreats (each sourcing a rapid Fairbridge-type SL rise) and intervening readvances. In East Antarctica at Denman Glacier (seemingly 'primed' for a MICI event in the near future; see Section 5), "possible Late Holocene readvance of the region's ice sheet" (King et al., 2022, p. 1) is indicated by GPS data that show subsidence, rather than the uplift predicted by glacio-isostatic models that assume uninterrupted Holocene retreat. Fears of future collapse of the entire West Antarctic Ice Sheet (e.g. Naughten et al., 2023), which would raise SL ~ 5m (Morlighem et al., 2020), are assuaged by the West Antarctic Ice Sheet Divide Ice Core, in which all annual layers for the last 31ky have been identified (Sigl et al., 2016), implying that none of the Holocene Fairbridge-type SL rises involved full collapse of this ice sheet.

3. Rottnest ice-collapse event caused by global warming?

The MICI event inferred to have supplied the Rottnest SL rise is attributed here to a known warming event. The rise began ~430AD (Higgs 2024, 2025b), only ~30y after

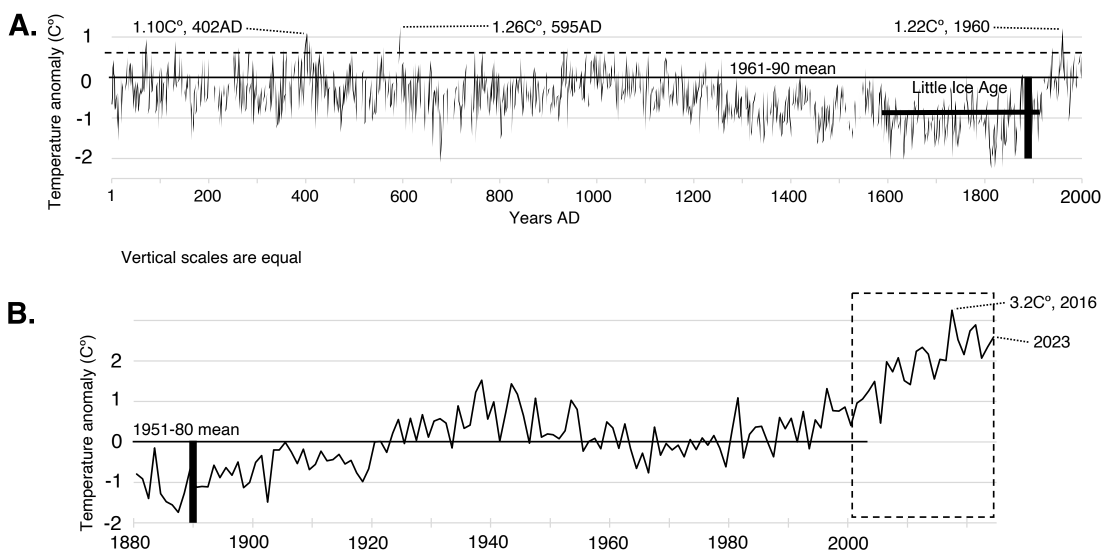

Figure 1. (A) 1-2000AD Arctic (latitude 60-90ºN) multi-proxy mean annual sea-surface- and terrestrial near-surface-air temperature (C° deviations from 1961-1990 mean). Data from McKay and Kaufman (2014), Excel Data File "Reconstruction v1.1.1" at www.ncei.noaa.gov/access/paleo-search/study/16973 . Note 402AD warm spike, within a 12-year (398-409AD) period in which an unrivalled 8 years (5 consecutive) were >0.6C° warmer (dashed line) than the 1961-90 mean. The 595 and 1960 peaks were higher, but both warm intervals were briefer. By plotting 30-year running-means, the 402 peak is highest (and it shifts to 395; see Figure 2B). (B) 1800-2023 thermometer-measured Arctic (64-90ºN) annual mean land-ocean near-surface air temperature (C° deviations from 1951-1980 mean; NASA data at https://data.giss.nasa.gov/gistemp/tabledata_v4/ZonAnn.Ts+dSST.txt. The 1900-2023 portion of this graph also appears in Ballinger et al. (2023, fig. 1, GISTEMP v4 graph). Note: (i) the years 2001 onward (dashed black box), including the warmest years in the record, are not represented in graph A, which ends at 2000 (see also Figure 3); and (ii) in both data-sets, the annual means for 1951-1980 and 1961-1990 are equal, i.e. the zero baselines in A and B are the same. To aid comparison, black vertical bar at 1890AD in both graphs has the same temperature range, 0 to -2C°. In A, the heavy horizontal bar spanning 1680-1920 is the Little Ice Age (e.g. https://en.wikipedia.org/wiki/Little_Ice_Age; cf. Figure 2).

the start of an Arctic 12-y warm period (398-409AD; peak 402AD; Figure 1A). Only twice in the 1-2000AD period was the 402AD peak temperature exceeded, but the *duration* of warmth in each case was less (Figure 1A), only 4 and 5y (from data-source given in Figure 1A caption). The 402AD spike coincides with a 400-450AD warm episode on a *global* averaged proxy-temperature graph (PAGES2k, 2017, fig. 7a, b, 25- and 50y-bin averages; contrast PAGES2k, 2019, fig. 1a, different method), but is not evident on a graph for Antarctica (May, 2017, fig. 3A).

Only ~100y before the Arctic temperature spike, the Sun's strongest magnetic grand-maximum (GM) of the interval 1-1885AD occurred, lasting several decades and peaking at ~305AD (Figure 2A). This probable correlation, and other apparent matches between solar-magnetic- and Arctic-temperature extremes, both high and low, and the matching *overall* decline of solar output and temperature (again time-lagged; Figure 2), suggest likely causation. The ~100y lag may reflect ocean thermal inertia, which "causes climate change to lag behind any changes in external forcing ... (by) ... many decades" (Wigley, 2005, p. 1766). The additional lag of ~30y, between the start of the Arctic hot-spike (398AD) and the Rottnest onset (~430AD), is attributed here to global 'conveyor-belt' thermohaline circulation (Marshall and Speer, 2012), specifically the time delay for north-travelling (in the conveyor) Atlantic surface water, somewhat 'overwarmed' by the GM (fewer clouds; Svensmark, 2007), to sink in the Arctic downwelling zone (Marshall and Speer, 2012, fig. 1), then travel south to Antarctica, eventually upwelling and circling the continent (their fig. 1 and box 1 diagram), unleashing ice-collapse by MICI. This model requires that Arctic downwelling continued throughout the warm interval, despite inevitable ocean-surface warming and higher meltwater influx, both tending to hinder downwelling by lowering the surface-water density, suggesting that this effect was compensated or outweighed by an increase in the salinity of Atlantic surface water arriving (from lower latitudes with raised evaporation) in the northbound upper limb of the 'conveyor' (cf. Rahmstorf, 2006, elaborating on Stommel, 1961).

Previous authors have shown a correlation between solar activity and Holocene climate variations (Bond et al., 2001; Usoskin et al., 2005; Perry, 2007; Eichler et al., 2009), with lag-times ranging from undetectable to ~100y. The critical solar variable is the magnetic flux (Svensmark, 2007), as opposed to the total solar irradiance, which varies in lockstep with the former, but its variations are far smaller (e.g. see figure 1 of Benevolenskaya and Kostuchenko, 2013). In good agreement with the Rottnest solar/SL lag of ~130y (see above), simulated Atlantic SL variations (climate-controlled) for the last 1.5ky appear to match solar variations, with a lag of ~125y (van de Plassche et al., 2003).

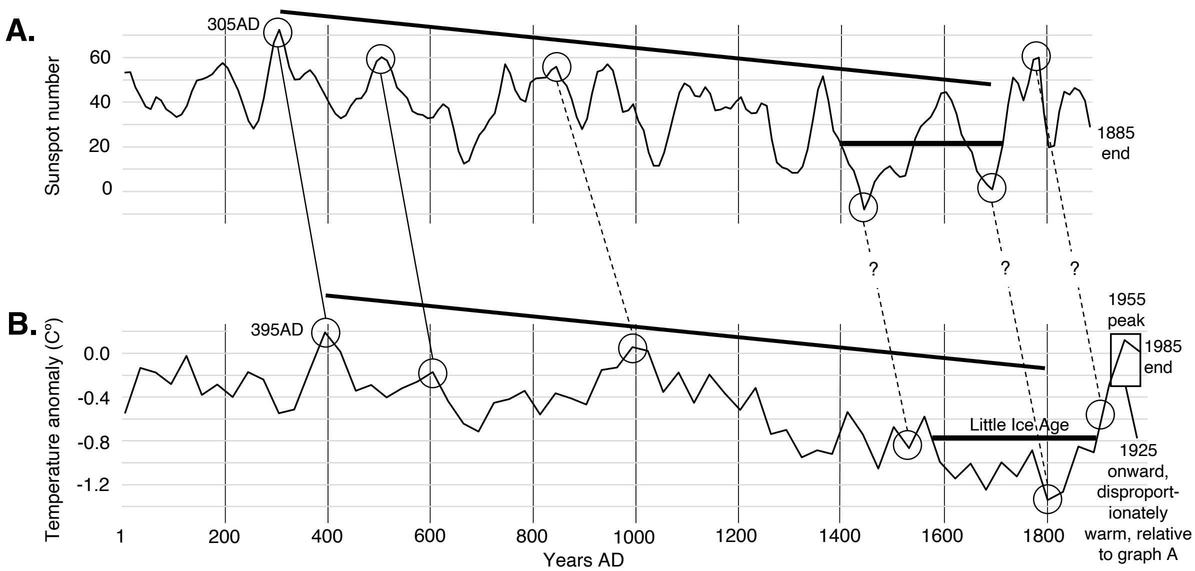

Figure 2. Fair correlation since 1AD between: (A) reconstructed sunspot numbers (data from Wu et al., 2018; 10-year sample interval), a proxy for solar magnetic output (e.g. fig. 3 of Lockwood et al., 1999); and (B) Arctic (latitude 60-90ºN) 30-year averages of mean annual sea-surface- and terrestrial near-surface-air-temperature excess (C° deviations from 1961-1990 mean), multi-proxy (same source as Figure 1B). Note the 90y lag between the two highest peaks on the graphs (305 and 395AD). Other peaks cross-match with a similar offset (dashed lines indicate less confidence), as do the overall decline in both solar output and Arctic temperature (sloping heavy bars), and the matching periods of exceptionally low solar output and Little Ice Age exceptionally low temperature (heavy horizontal bars). A solar cause of the Little Ice Age was proposed by Denton and Karlén (1973).

After the 400-412AD Arctic warm spike, the earlier of the two even-warmer spikes (peak temperature at 595AD; Figure 1A) failed to produce a metre-scale, Rottnest-lookalike SL rise. A possible reason is insufficient *duration* (only 4y) of Arctic excess-temperature above a 'MICI threshold' value of, say, 0.6C° warmer than the 1961-90 mean (dashed line in Figure 1A). The implication is that unleashing a MICI event requires more than 4y of 'overwarmed' ocean water upwelling (to fully melt the buttressing ice shelves and retreat the glacier enough to produce ice cliffs sufficiently high, if not already; see Section 2) and less than 12y (duration of the Rottnest-driving Arctic warm spike). Similarly, the subsequent hot-spike (peak 1960, Figure 1A), lasting only 5y, produced no Rottnest-like rise starting ~30y (lag) later. The evident joint importance of Arctic excess-temperature value *and* duration is effectively illustrated by plotting 30y-average temperatures instead of annual values, whereupon the ~400AD event becomes the warmest (compare Figures 1A and 2B); the same applies to 10y averages (McKay and Kaufman, 2014, fig. 2d).

4. Cause of post-Rottnest regression

The near-immediate onset of the post-Rottnest SL fall (~3m spanning ~550-900AD in figure 1 of Higgs, 2025b; cf. ~2m spanning ~500-550AD in Fairbridge and Hillaire-Marcel, 1977, fig. 2), within decades of the Rottnest rise ending (~500AD; Higgs, 2025b, figure 1), suggests that the causative ice-collapse event also guaranteed an ensuing fall. The same applies to all of the Holocene SL oscillations on the Fairbridge Curve: each rise is followed by a fall of similar magnitude (1-5m), with high- and lowstands disposed roughly symmetrically above and below modern mean SL (see original Fairbridge Curve in Fairbridge, 1961, fig. 15).

An intrinsic SL-fall mechanism is easier to visualize for a MICI event than for a MISI, as follows. MICI events involve (require) complete loss of ice shelves before the glacier can undergo cliff failure. Antarctica's ice shelves currently have a vast total area, 1.4 x 10^6km^2, about 10% as large as the continent (Andreasen et al., 2023, table 1 and fig. 1). Removal of an entire ice-shelf sector would raise summertime humidity in the adjacent coastal zone, due to exposure of bare ocean (except winter sea-ice), albeit strewn with tall icebergs (cf. Wise et al., 2017, fig. 4b). In particular, glacier retreat in the Ross- and Weddell Sea sectors (see Section 2) by MICI rather than MISI would imply complete loss of the huge Ross- and Filchner-Ronne ice shelves (area 0.9 x 10^6km^2, equalling France and Germany combined), raising humidity in the very long coastal sectors adjacent. The higher humidity would increase snowfall, lowering SL. (Present-day Antarctica is a 'polar desert' with extremely low humidity.) Adding to the humidity, the abundant tall icebergs released by MICI would warm (sic) the offshore surface water. For the proposed mechanism to generate enough additional snowfall to lower SL by as much as 2-3m would possibly require total removal of the ice shelf around much or all of Antarctica's perimeter.

5. Another metre-scale sea-level rise imminent?

Due to anthropogenic global warming (IPCC, 2021), Arctic average land-and-sea surface-air temperature has, every year since 2005, exceeded the 402AD peak, by up to 2C^{o} (sic; Figures 1, 3), and for longer (20y to date) than the entire 398-409AD (12y) warm interval to which the Rottnest transgression is here attributed (see Section 3). Thus, another rapid, metre-scale SL rise is predictable, beginning by ~2035 (2005 plus ~30y lag; see Section 3). Before 2100, the time-lagged effect of the Sun's latest GM, which spanned ~1935-2005 (Rohde, 2023) and was even stronger than the ~300AD GM (Wu et al., 2018, fig. 14), will begin to exacerbate the warming.

Supporting the prediction of a MICI event beginning within ~10y from today (2025), and indicating that upwelling ocean water is already warmer than usual, Antarctic indicators of possible imminent glacier collapse are plentiful, both in the west and the east. In West Antarctica, over the past few decades, the intensely monitored Thwaites Glacier and PIG "have shown accelerated ice flow, rapid thinning, and fast retreat of the grounding line" (Hillenbrand et al., 2013, p. 35). PIG's grounding line has already receded from a seabed ridge on which "the glacier was partially pinned" prior to 1973 (Graham et al. 2013, p. 1357 and fig. 1b), and is now on a retrograde bed (Rignot et al., 2014). Incipient MISI (sic) retreat has been inferred at PIG and Thwaites (Favier et al. 2014; Joughin et al., 2014; Rignot et al., 2014; all of these publications predate the MICI concept). PIG's grounding-line subsea depth was already ~900-1100m in 2011 (Rignot et al., 2014, fig. 3a, b), exceeding the MICI threshold (~700m, after ice-shelf has gone; see Section 2). Moreover, PIG's bed-depth exceeds the MICI threshold for >100km upstream of the present grounding line (Bingham et al., 2017, fig. 1c). Thwaites grounding line's subsea depth, ~500m (Rignot et al., 2014, fig. 3c, d), is hypothetically insufficient for a MICI event. However, having retreated, in places, up to ~10km in 11y (2000-2011; Rignot et al., 2014, fig. 1), the grounding line only needs to retreat ~10km more to reach depths >700m locally (Rignot et al., 2014, fig. 3c, d). At Thwaites, "We do not find major bumps in bed topography upstream of the current grounding line that could stop the grounding line retreat, except for two prominent ridges ~35 and 50km upstream" (Morlighem et al., 2020, p. 3). Thus, PIG and Thwaites, especially the former, seem primed for a MICI event, as soon the remainder of their ice shelves disintegrates. Both shelves shrank between 2009 and 2019 (Andreasen et al., 2023, fig. 1). Final disappearance of what remains of Thwaites' ice shelf is considered "very likely" to begin "within the next decade" (Wild et al., 2022, p. 407).

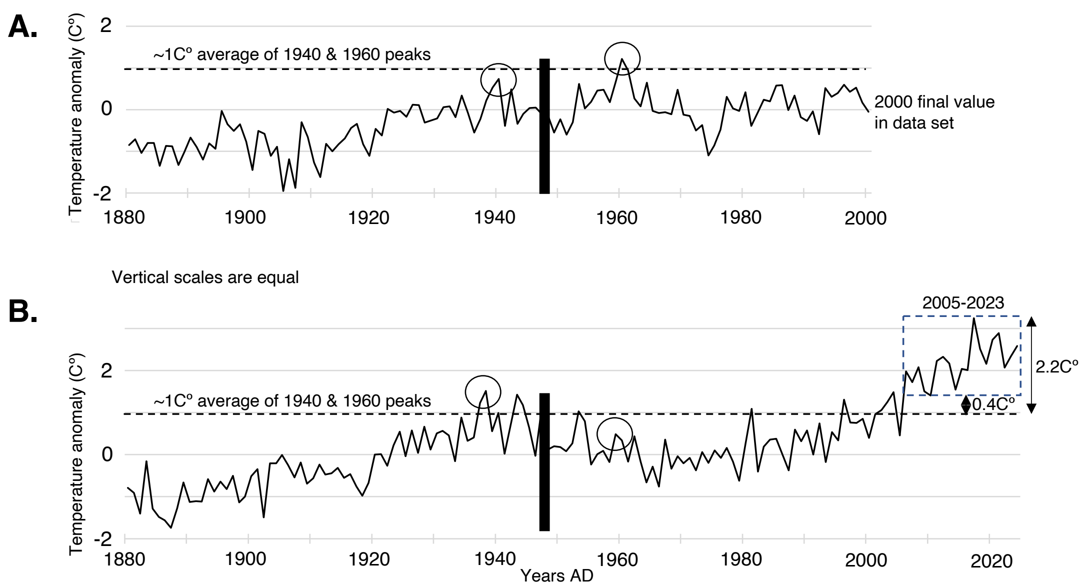

Figure 3. Graphs of Arctic post-1880 temperatures based on (A) proxies and (B) thermometers. Same sources as in Figure 1. The graphs show good resemblance in the period of overlap (1880-2000), and near-identical temperature spans (~3.2Cº; black bars), though slightly displaced (0.2-0.3Cº). The magnitudes of the ~1940 and ~1960 peaks (four circles) are 'reversed'. However, in both cases, the peak values average ~1Cº (dashed lines), nearly equal to the 402AD peak (1.1Cº; Figure 1). From 2005 to 2023 (total 19 years), this value was *exceeded continuously, by 0.4Cº to 2.2Cº* (dashed box).

Similarly, East Antarctica has a number of glaciers apparently ripe for a MICI event. The grounding lines of Smith and Evans glaciers are on retrograde slopes and already >700m deep (Morlighem et al., 2020, fig. 2). Denman Glacier is accelerating and its grounding line is retreating on a retrograde slope (Miles et al., 2021). According to Brancato et al. (2020, p. 674), "the potential exists for Denman Glacier to retreat irreversibly into the deepest, marine-based basin in Antarctica". The grounding line retreated ~5km from 1996 to 2018 (Brancato et al., 2020); its subsea depth varies, across the glacier, from ~1,000m (Miles et al., 2021, fig. 1) to >2km (Brancato et al., 2020). "Given its bed topography and the geological evidence that Denman Glacier has retreated substantially in the past, its recent grounding line retreat and ice flow acceleration suggest that it could be poised to make a significant contribution to sea level in the near future" (Miles et al., 2021, p. 663). Fronting Denman Glacier, Shackleton Ice Shelf underwent a comparatively small growth between 2009 and 2019 (Andreasen et al., 2023, fig. 1). However, ice shelves can disintegrate very quickly, within a few weeks, as evidenced by Sectors A and B of Larsen Ice Shelf in 1995 and 2002 respectively (Scambos et al., 2004).

Antarctic glaciers whose grounding line is deeper than 700m (Morlighem et al., 2020) include four whose shelf underwent 2009-19 shrinkage (Andreasen et al., 2023, fig. 1), namely Mertz, Pine Island, Thwaites and Totten (cross-flow widths respectively ~10, 30, 80 and 25km at the grounding line; Morlighem et al., 2020, figs 1, 2, S6, S8); and eight whose ice shelf expanded, namely Byrd (Ross Ice Shelf), Denman (Shackleton), Evans (Ronne), Mellor (Amery), Ninnis, Recovery (Filchner), Slessor (Filchner) and Smith (Crosson) (~15, 10, 30, 15, 15, 60, 60 and 10km).

Seventy years ago, Kuenen (1954, p. 153) perceptively wrote: "The sword of Damocles hanging over the Low Countries is formed by the waters pent up in the ice sheets of Greenland and Antarctica". The same applies to other low-lying nations, such as Bangladesh and all of the world's atolls.

References

An, L., Rignot, E.; Elieff, S.; Morlighem, M.; Millan, R.; Mouginot, J., et al., 2017. Bed elevation of Jakobshavn Isbr., West Greenland, from high-resolution airborne gravity and other data. *Geophysical Research Letters*, 44, doi: 10.1002/2017GL073245

Andreasen, J.R.; Hogg, A.E., and Selley, H.L., 2023. Change in Antarctic ice shelf area from 2009 to 2019. *The Cryosp*here, 17, 2059–2072.

Benevolenskaya, E.E. and Kostuchenko, I.G., 2013. The total solar irradiance, UV emission and magnetic flux during the last solar cycle minimum. Journal of Astrophysics, 2013(368380), doi: org/10.1155/2013/368380

Bindschadler, R.A.; Roberts, E.P., and Almut Iken, A., 1990. Age of Crary Ice Rise, Antarctica, determined from temperature-depth profiles. *Annals of Glaciology*, 14, 13-16.

Bingham, R.G.; Vaughan, D.G.; King, E.C.; Davies, D.; Cornford, S.L.; Smith, A.M., et al., 2017. Diverse landscapes beneath Pine Island Glacier influence ice flow. *Nature Communications*, 8(1618), doi: 10.1038/s41467-017-01597-y

Bond, G.; Kromer, B.; Beer, J.; Muscheler, R.; Evans, M.N.; Showers, W., et al., 2001. Persistent solar influence on North Atlantic climate during the Holocene. *Science*, 294, 2130-2136.

Bondzio, J.H.; Morlighem, M.; Seroussi, H.; Wood, M., and Mouginot, J., 2018. Control of ocean temperature on Jakobshavn Isbræ's present and future mass loss. *Geophysical Research Letters*, 45, 12,912–12,921,

Braddock, S.; Hall, B.L.; Johnson, J.S.; Balco, G.; Spoth, M.; Whitehouse, P.L., et al., 2022. Relative sea-level data preclude major late Holocene ice-mass change in Pine Island Bay. *Nature Geoscience*, 15, 568–572.

Bradley, S.L.; Richard C.A. Hindmarsh, R.C.A.; Whitehouse, P.L.; Bentley, M.J., and King, M.A., 2015. Low post-glacial rebound rates in the Weddell Sea due to Late Holocene ice-sheet readvance. *Earth and Planetary Science Letters*, 413, 79–89.

Brancato, V.; Rignot, E.; Milillo, P.; Morlighem, M.; Mouginot, J.; An, L., et al., 2020. Grounding line retreat of Denman Glacier, East Antarctica, measured with COSMO-SkyMed radar interferometry data. Geophysical Research Letters, 47(e2019GL086291), doi: org/10.1029/2019GL086291

DeConto, R.M. and Pollard, D., 2016. Contribution of Antarctica to past and future sea-level rise. *Nature*, 531, 591-597.

Denton, G.H. and Karlén, W., 1973. Holocene climatic variations – their pattern and possible cause. *Quaternary Research*, 3, 155-174.

Eichler, A.; Olivier, S.; Henderson, K.; Laube, A.; Beer, J.; Papina, T., et al., 2009. Temperature response in the Altai region lags solar forcing. *Geophysical Research Letters*, 36(L01808), doi: 10.1029/2008GL035930

Fairbridge, R.W., 1961. Eustatic changes in sea level. *In:* Ahrens, L.H.; Press, F.; Rankama, K., and Runcorn, S.K. (eds.). *Physics and Chemistry of the Earth, volume 4*, London: Pergamon, pp. 99–185.

Fairbridge, R.W., 1976. Shellfish-eating Preceramic Indians in coastal Brazil. *Science*, 191, 353-359.

Fairbridge, R.W. and Hillaire-Marcel, C., 1977. An 8,000-yr palaeoclimatic record of the 'Double-Hale' 45-yr solar cycle. *Nature*, 268, 413-416.

Favier, L.; Durand, G.; Cornford, S.L.; Gudmundsson, G.H.; Gagliardini, O.; Gillet-Chaulet, F.; Zwinger, T.; Payne, A.J., and Le Brocq, A.M., 2014. Retreat of Pine Island Glacier controlled by marine ice-sheet instability. Nature Climate Change, 4, 117-121.

Graham, A.G.C.; Dutrieux, P.; Vaughan, D.G.; Nitsche, F.O.; Gyllencreutz, R.; Greenwood, S.L., et al., 2013. Seabed corrugations beneath an Antarctic ice shelf revealed by autonomous underwater vehicle survey: origin and implications for the history of Pine Island Glacier. *Journal Of Geophysical Research: Earth Surface*, 118, 1356–1366.

Graham, A.G.C.; Jakobsson, M.; Nitsche, F.O.; Larter, R.D.; Anderson, J.B.; Hillenbrand, C.-D., et al., 2016. Submarine glacial-landform distribution across the West Antarctic margin, from grounding line to slope: the Pine Island–Thwaites ice-stream system. *In:*

Dowdeswell, J.A.; Canals, M.; Jakobsson, M.; Todd, B. J.; Dowdeswell, E. K., and Hogan, K.A. (eds.), *Atlas of Submarine Glacial Landforms: Modern, Quaternary and Ancient*. Geological Society, London, Memoirs, 46, 493–500.

Graham, A.G.C.; Wåhlin, A.; Hogan, K.A.; Nitsche, F.O.; Heywood, K.J.; Totten, R.L., et al., 2022. Rapid retreat of Thwaites Glacier in the pre-satellite era. *Nature Geoscience,* 15, 706–713.

Higgs, R., 2024. British archaeology verifies 5th-Century rapid multi-metre sea-level rise and portends another before 2100. European Geosciences Union, 2024 General Assembly, Vienna, https://doi.org/10.5194/egusphere-egu24-1322 (abstract and downloadable poster).

Higgs, R., 2025a. Holocene oscillatory sea level: literature review and implications for imminent anthropogenic multi-metre transgression. *Non-peer-reviewed preprint at EarthArXiv,* DOI: XX

Higgs, R., 2025b. Geological review of English coastal archaeological evidence portending multi-metre sea-level rise by 2100. *Non-peer-reviewed preprint at ArXiv,* DOI: XX

Hillenbrand, C.-D.; Kuhn, G.; Smith, J.A.; Gohl, K.; Graham, A.G.C.; Larter, R.D., et al., 2012. Grounding-line retreat of the West Antarctic Ice Sheet from inner Pine Island Bay. *Geology*, 41, 35-38.

Hogan, K.A.; Warburton, K.L.P.; Graham, A.G.C.; Neufeld, J.A.; Hewitt, D.R.; Dowdeswell, J.A., and Larter, R.D., 2023. Towards modelling of corrugation ridges at ice-sheet grounding lines. *The Cryosphere*, 17, 2645–2664

IPCC, 2019. Chapter 3: Polar regions. *In: Special Report on the Ocean and Cryosphere in a Changing Climate.* Cambridge and New York: Cambridge University Press, pp. 203–320.

IPCC, 2021. Summary for policymakers. *In:* Climate Change 2021: The Physical Science Basis. *Contribution of Working Group I to the Sixth Assessment Report of the Intergovernmental Panel on Climate Change*. Cambridge and New York: Cambridge University Press, pp. 3-31.

Jakobsson, M.; Anderson, J.B.; Nitsche, F.O.; Dowdeswell, J.A.; Gyllencreutz, R.; Kirchner, N., et al., 2011. Geological record of ice shelf break-up and grounding line retreat, Pine Island Bay, West Antarctica. *Geology*, 39, 691–694.

Jakobsson, M.; Anderson, J.B.; Nitsche, F.O.; Gyllencreutz, R.; Kirshner, A.E.; Kirchner, N., et al., 2012. Ice sheet retreat dynamics inferred from glacial morphology of the central Pine Island Bay Trough, West Antarctica. *Quaternary Science Reviews,* 38, 1-10

Jakobsson, M. and Anderson, J.B., 2016. Corrugation ridges in the Pine Island Bay glacier trough, West Antarctica. *In:* Dowdeswell, J.A.; Canals, M.; Jakobsson, M.; Todd, B. J.; Dowdeswell, E. K., and Hogan, K.A. (eds.), *Atlas of Submarine Glacial Landforms: Modern, Quaternary and Ancient*. Geological Society, London, Memoirs, 46, 265-266.

Johnson, J.S.; Bentley, M.J.; Smith, J.A.; Finkel, R.C.; Rood, D.H.; Gohl, K., et al., 2014. Rapid Thinning of Pine Island Glacier in the Early Holocene. *Science*, 343, 999-1001.

Johnson, J.S.; Venturelli, R.A.; Balco, G.; Allen, C.S.; Braddock, S.; Campbell, S., and Goehring, B.M., 2022. Review article: Existing and potential evidence for Holocene grounding line retreat and readvance in Antarctica. *The Cryosphere,* 16, 1543–1562.

Jones, R.S.; Mackintosh, A.N.; Norton, K.P.; Golledge, N.R.; Fogwill, C.J.; Kubik, et al., 2015. Rapid Holocene thinning of an East Antarctic outlet glacier driven by marine ice sheet instability. *Nature Communications*, 6(8910), doi: 10.1038/ncomms9910

Joughin, I.; Smith, B.E., Medley, B., 2014. Marine Ice Sheet Collapse Potentially Under Way for the Thwaites Glacier Basin, West Antarctica. *Science*, 344, 735-738.

King, M.A.; Watson, C.S., and White, D., 2022. GPS rates of vertical bedrock motion suggest late Holocene ice-sheet readvance in a critical sector of East Antarctica. *Geophysical Research Letters*, 49(e2021GL097232), doi: org/10.1029/2021GL097232

Kingslake, J.; R. P. Scherer, R.P.; Albrecht, T.; Coenen, J.; Powell, R.D.; Reese, R., et al., 2018. Extensive retreat and re-advance of the West Antarctic Ice Sheet during the Holocene. *Nature*, 558, 430–434.

Kuenen, Ph. H., 1954. Eustatic changes of sea-level. *Geologie en Mijnbouw*, 16, 148-155.

Lockwood, M.; Stamper, R., and Wild, M.N., 1999. A doubling of the Sun's coronal magnetic field during the past 100 years. *Nature*, 399, 437-439.

Marshall, J. and Speer, K., 2012. Closure of the meridional overturning circulation through Southern Ocean upwelling. *Nature Geoscience*, 5, 171-180.

May, A., 2017. *A Holocene Temperature Reconstruction Part 1: the Antarctic.* Webpage, accessed 5th February 2025. https://andymaypetrophysicist.com/2017/05/31/a-holocene-temperature-reconstruction-part-1-the-antarctic/

McKay, N.P. and Kaufman, D.S., 2014. An extended Arctic proxy temperature database for the past 2,000 years. *Nature Scientific Data*, 1(140026), doi: 10.1038/sdata.2014.26

Miles, B.W.J.; Jordan, J.R.; Stokes, C.R.; Jamieson, S.S.R.; Gudmundsson, G.H., and Jenkins, A., 2021. Recent acceleration of Denman Glacier (1972–2017), East Antarctica, driven by grounding line retreat and changes in ice tongue configuration. *The Cryosphere,* 15, 663–676.

Morlighem, M.; Williams, C.N.; Rignot, E.; An, L.; Arndt, J.E.; Bamber, J.L., et al., 2017. BedMachine v3: complete bed topography and ocean bathymetry mapping of Greenland from multibeam echo sounding combined with mass conservation. *Geophysical Research Letters,* 44, 11,051–11,061.

Morlighem, M.; Rignot, E.; Binder, T.; Blankenship, D.; Drews, R.; Eagles, G., et al., 2020. Deep glacial troughs and stabilizing ridges unveiled beneath the margins of the Antarctic ice sheet. *Nature Geoscience*, 13, 132-137.

Morlighem, M.; Goldberg, D.; Barnes, J.M.; Bassis, J.N.; Benn, D.I.; Crawford, A.J., et al., 2024. The West Antarctic Ice Sheet may not be vulnerable to marine ice cliff instability during the 21st century. *Science Advances*, 10(34), doi: 10.1126/sciadv.ado7794

Naughten, K.A.; Holland, P.R., and De Rydt, J., 2023. Unavoidable future increase in West Antarctic ice-shelf melting over the twenty-first century. *Nature Climate Change*, 13, 1222–1228.

Needell, C. and Holschuh, N., 2023. Evaluating the retreat, arrest, and regrowth of Crane Glacier against marine ice cliff process models. *Geophysical Research Letters*, 50(e2022GL102400), doi: org/10.1029/2022GL102400

PAGES2k Consortium, 2017. A global multiproxy database for temperature reconstructions of the Common Era. *Nature Scientific Data*, 4(170088), doi: 10.1038/sdata.2017.88

PAGES2k Consortium, 2019. Consistent multidecadal variability in global temperature reconstructions and simulations over the Common Era. *Nature Geoscience*, 12, 643–649.

Pattyn, F., 2018. The paradigm shift in Antarctic ice sheet modelling. *Nature Communications*, 9(2728), doi: 10.1038/s41467-018-05003-z

Perry, C.A., 2007. Evidence for a physical linkage between galactic cosmic rays and regional climate time series. *Advances in Space Research*, 40, 353–364.

Pollard, D.; DeConto, R.M., and Alley, R.B., 2015. Potential Antarctic Ice Sheet retreat driven by hydrofracturing and ice cliff failure. *Earth and Planetary Science Letters*, 412, 112-121.

Rahmstorf, S., 2006. Thermohaline ocean circulation. *In:* Elias, S.A. (ed.), *Encyclopedia of Quaternary Sciences*. Amsterdam: Elsevier, pp. 1-10.

Rebesco, M.; Domack, E.; Zgur, F.; Lavoie, C.; Leventer, A.; Brachfeld, S., et al., 2014. Boundary condition of grounding lines prior to collapse, Larsen-B Ice Shelf, Antarctica. *Science*, 345, 1354-1358.

Rignot, E. and Mouginot, R., 2012. Ice flow in Greenland for the International Polar Year 2008–2009. *Geophysical Research Letters*, 39(L11501), doi: 10.1029/2012GL051634

Rignot, E.; Mouginot, J.; Morlighem, M.; Seroussi, H., and Scheuchl, B., 2014. Widespread, rapid grounding line retreat of Pine Island, Thwaites, Smith, and Kohler glaciers, West Antarctica, from 1992 to 2011. *Geophysical Research Letters*, 41, 3502–3509.

Rohde, R.A., 2023. *400 years of sunspot observations. Sunspot chart, 1600-2022AD*. Wikipedia webpage, accessed 5th February 2025, https://en.m.wikipedia.org/wiki/File:Sunspot_Numbers.png

Scambos, T.A.; Bohlander, J.A.; Shuman, C.A., and Skvarca, P., 2004. Glacier acceleration and thinning after ice shelf collapse in the Larsen B embayment, Antarctica. Geophysical Research Letters, 31(L18402), doi: 10.1029/2004GL020670

Siegert, M.; Ross, N.; Corr, H.; Kingslake, J., and Hindmarsh, R., 2013. Late Holocene ice-flow reconfiguration in the Weddell Sea sector of West Antarctica. *Quaternary Science Reviews,* 78, 98-107.

Siegert, M.J., Kingslake, J., Ross, N., Whitehouse, P.L., Woodward, J., Jamieson, S.S.R., et al., 2019. Major ice sheet change in the Weddell Sea Sector of West Antarctica over the last 5,000 years. *Reviews of Geophysics*, 57, 1197-1223.

Sigl, M.; Fudge, T.J.; Winstrup, M.; Cole-Dai, J.; Ferris, D.; McConnell, J.R., et al., 2016. The WAIS Divide deep ice core WD2014 chronology – Part 2: Annual-layer counting (0–31ka BP). *Climate of the Past,* 12, 769–786.

Stommel, H. 1961. Thermohaline convection with two stable regimes of flow. *Tellus*, 13(2), 224-230.

Straneo, F.; Hamilton, G.S.; Stearns, L.A., and Sutherland, D.A., 2016. Connecting the Greenland Ice Sheet and the ocean: a case study of Helheim Glacier and Sermilik Fjord. *Oceanography*, 29, 22-33.

Sun, S.; Pattyn, F.; Simon, E.G.; Albrecht, T.; Cornford, S.; Calov, R., et al., 2021. Antarctic ice sheet response to sudden and sustained ice-shelf collapse (ABUMIP). *Journal of Glaciology*, *66*, 891–904.

Svensmark, H., 2007. Cosmoclimatology: a new theory emerges. *Astronomy and Geophysics*, 48(1), 1.18-1.24.

Usoskin, I. G.; Schüssler, M.; Solanki, S. K., and Mursula, K., 2005. Solar activity, cosmic rays, and Earth's temperature: a millennium-scale comparison. *Journal of Geophysical Research*, 110(A10102), doi: 10.1029/2004JA010946

van de Plassche, O.; van der Schrier, G.; Weber, S.L.; Gehrels, W.R., and Wright, A.J., 2003. Sea-level variability in the northwest Atlantic during the past 1500 years: a delayed response to solar forcing? *Geophysical Research Letters*, 30(18), 1921, doi: 10.1029/2003GL017558

Walker, M., and 18 others, 2009. Formal definition and dating of the GSSP (Global Stratotype Section and Point) for the base of the Holocene using the Greenland NGRIP ice core, and selected auxiliary records. *Journal of Quaternary Science*, 24, 3–17.

Wigley, T.M.L., 2005. The climate change commitment. *Science*, 307(5716), 1766-1769, doi: 10.1126/science.1103934

Wild, C.T.; Alley, K.E.; Muto, A.; Truffer, M.; Scambos, T.A., and Pettit, E.C., 2022. Weakening of the pinning point buttressing Thwaites Glacier, West Antarctica. *The Cryosphere,* 16, 397–417.

Wise, M.G.; Julian A. Dowdeswell, J.A.; Jakobsson, M., and Larter, R.D., 2017. Evidence of marine ice-cliff instability in Pine Island Bay from iceberg-keel plough marks. *Nature*, 550(7677), 506-510.

Wu, C.J.; Usoskin, I.G.; Krivova, N.; Kovaltsov, G.A.; Baroni, M.; Bard, E., and Solanki, S.K., 2018. Solar activity over nine millennia: a consistent multi-proxy reconstruction? *Astronomy and Astrophysics*, 615(A93), doi: 10.1051/0004-6361/201731892